Analysis of expansion within a pressure inflated section of a simplified urethral model

A. Bhave*, K. Möller*.

** Institute of Technical Medicine (ITeM), Furtwangen University, 78054 Villingen-Schwenningen, Germany (Tel:+49 7720-307-4785; e-mail: bha@hs-furtwangen.de)*

Abstract: A new inflatable sensor-actuator system is being developed to analyze the in-vivo biomechanical properties of the urethra of a male human. It could provide decision-aids to urologists while treating issues like urethral strictures. Models that could simulate the biomechanical variations of the urethra are important to evaluate the capabilities of the system under development. For the initial study, a simplified axisymmetric Finite Element Method 'tube' model was generated. To simulate an ideal inflating actuator (balloon) within this urethra model, a pressure was applied on the inner wall of the tube. From the region over which the pressure was applied, 'sensor' measurements were taken from the 'top' plane, 'middle' plane and a plane lying between these two. The resulting pressure-circumference and pressure-(wall)thickness responses at these measurement planes were determined. A hyperelastic response attributable to biological tissues was obtained. It was found that the resultant circumferential extension and thickness varies at different planes during the actuator inflation. After inflating at the highest chosen pressure, from the initial inner circumference of 25mm, final extensions ranging 45mm to 63mm for the peripheral plane were obtained. Similarly, extensions ranging from 48mm to 68mm were obtained for the other two planes. The pressure-circumference response at the plane lying on the periphery of the inflated region was found to be less compliant than the plane in the center for the model. A range of biomechanical responses were able to be achieved by performing a parametric variation for the chosen mathematical model and geometry in consideration. The study indicates that a larger dataset can be generated to further model a variety of urethral biomechanical responses. These initial simulations provide important information for identification tasks related to the current development. The results show that simulations could be a prospective way to test new sensors prior to real experiments.

Keywords: urethra, simulation, in-vivo, biomechanics, strictures, sensor

1.INTRODUCTION

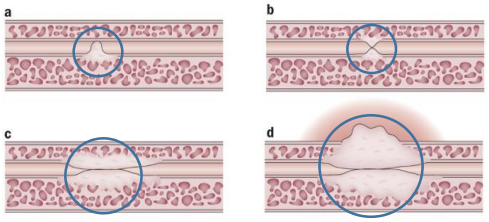

Figure 1. Longitudinal section of strictured urethra (encircled in blue)-examples. (Dr. Ali AL-Amiri et al., accessed 2020)

The 'urethra' is a tubular structure in the human genito-urinary tract that allows passage of urine and other fluids. Urethral stricture consists of tissue hardening and narrowing of the walls within the urethra. Constrictions may occur after injury to the epithelium of the urethral lumen and/or underlying spongy tissue (Fig. 1). This can cause narrowing and hardening of the urethral wall primarily due to body repair mechanism which obstructs passage of fluids causing incontinence (Hampson, McAninch and Breyer, 2014; Mundy and Andrich, 2011).

A simple procedure is currently in practice whereby catheters of certain diameter are inserted in the urethra to open up the constriction. Although this provides relief to the patient in the short term, the recurrence of stricture or vessel failure is very high. Ultimately, a highly invasive surgical intervention may be required with its own set of issues. It is a challenge to determine the appropriate dilation/force which not only opens up the constriction, but also prevents any damage or recurrence of stricture. If a urologist could gain active information regarding the tissue properties, it may assist the stricture treatment procedure. At the core, understanding the behaviour of the urethral tissue and being able to predict it is unexplored and vital.

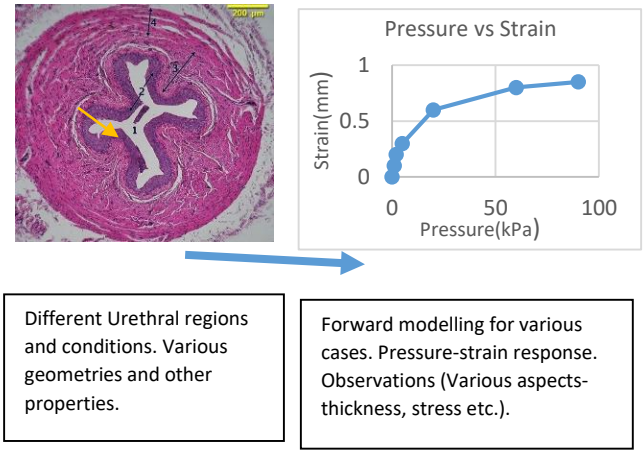

Figure 2. Forward Modelling. The modelling aims at creating Pressure v/s Strain or related graphs for variety of urethral conditions. Initial step in the identification process (Cross section image- BIO 202 Lab, copyrights-Savalli, Udo).

With a focus on these issues, at two research institutes of Furtwangen University, work on the project ILSA (Intra-Luminal Sensor Actuator) is being undertaken. An intra-luminal sensor coupled with a balloon actuator is being developed in this project which can provide pressure-stretch dynamics of the vessel, in-vivo, during a clinical procedure. From the sensor data being obtained during active manoeuvres performed intraluminal, the biomechanical behaviour and stretch limits of urethra could be predicted. This forms the main aim of the ILSA modelling group.

The forward modelling approach methodology is shown in short (Fig. 2). Forward modelling of the urethra is creating FEM models which are based on physics and causality ("forward identification") that could generate a biomechanical response given a stimulus. As the project is focussed more on understanding the in-vivo behaviour of the urethra, the first step is to perform the basic simulations to model behaviour based on the available anatomical and biomechanical data. The biomechanics of strictures is understudied. Stricture aspects may also be incorporated in certain simulations in addition to basic models(Bhave and Möller, 2021). It is mentioned earlier that the main motive of ILSA project- modelling group is to predict the nature of urethra from the stress-strain(pressure-extension) response form the sensor. Prediction/ identification of the actual urethra condition from the sensor data, can be understood as 'reverse' or 'inverse modelling'. This paper aims at exploring the different aspects of forward modelling and whether a dataset for simulation can be generated.

There have been certain studies undertaken by Masri et al. (Masri *et al.*, 2018), and Cunnane et al. (Cunnane *et al.*, 2021), that describe the biomechanical stress-strain relationship of the urethral tissues. It is known that there is structural variation within the urethra. The studies make histological observations and have performed planar and uniaxial tissue tests. Some of these authors have undertaken mathematical modelling of the urethra (Masri *et al.*, 2018; Natali *et al.*, 2016). Histology is suggestive that the complexity of the urethra and the distribution of a variety of tissues surrounding it make it a challenge for modelling. Mixed hypothetical formulations like inclusion of certain fibre orientations throughout the section of urethra have been considered in literature, which may not actually align to the actual histological observations. The current literature, however, lacks comparable in-vivo or pressure response studies. It was found that the urethra is a biomechanically not so well investigated.

Constitution of layers and fibres with different properties do cause a change in stresses and strains within the material (Gasser, Ogden and Holzapfel, 2006).As divergent from the multilayer modelling approach in arteries, a single layer consideration with appropriate anisotropic modelling could be sufficient to model and identify the overall stretch-strain response of the urethra. Various numerical outputs (a dataset) may be obtained by varying the model parameters. The simulations can help us understand the actual behaviour of tissues (Gasser, Ogden and Holzapfel, 2006; Holzapfel, Gasser and Ogden, 2000; Masri *et al.*, 2018).The aim is to generate simplified basic model and perform finite element analysis for some of urethral considerations.

2. METHODS

2.1 The mathematical description

COMSOL Multiphysics® is a general-purpose simulation software used for modelling designs, processes in fields of engineering, development, and scientific research. COMSOL's (v5.5) non-linear module add-on along with structure mechanics were used for the simulations (COMSOL, 2019)

Gasser et al., described a constitutive modelling for the arteries considering distribution of fibres. This equation is a stable modification derived from the classical Holzapfel Gasser Ogden model for arteries (Holzapfel, Gasser and Ogden, 2000). An anisotropic hyperelastic response could be generated in their implementations (Gasser, Ogden and Holzapfel, 2006). The strain energy density Equation defined by Gasser et al., was chosen as the mathematical equation for the modelling in this study. It is defined as follows:

$$\mathrm{W} = \mu(I_1 - 3) + \frac{k_1}{2k_2}\sum_{\alpha}\left(e^{k_2\left[\kappa(I_1)+(1-3*\kappa)\left(I_{fib}^{\alpha}\right)-1\right]^2} - 1\right) \quad (1)$$

As shown in (1), W is the strain energy density. μ is the the isotropic part constant of the neo-hookean material. I_1 is the first invariant of the tensor that includes the isotropic matrix. It is a trace of the Cauchy normal stresses on the tensor. The urethra tube has description of two fibre families. 'α'=1,2 depict these two fibre families and follow path of the cylinder geometry. The parameter $'\kappa'$ is a structural constant. This fibre networks are controlled by material properties $k_1$and k_2. $k_1$is the stress parameter expressed in kPa while k_2 is a dimensionless parameter that influences the exponential function. $(I_{\mathrm{fib}}^{\alpha})$ is the invariant which describes the stretch of the fibre family in consideration. The fibres contribute only when there a positive stretch in the fibres. i.e. I_{fib}^{α} and are greater than 1. Incompressibility condition was applied in COMSOL. Polyconvexity and stability conditions could be satisfied according to the author(Gasser and Holzapfel, 2007; Gasser, Ogden and Holzapfel, 2006; Holzapfel, Gasser and Ogden, 2000).

2.2 Finite Element Modelling (FEM) Cylindrical model creation and boundary conditions.

An axisymmetric model mode in COMSOL was used to create a hypothesized section of a urethra. A general geometry was followed for the simulations for the ILSA project urethra axisymmetric models. A cylinder with a thickness of the 5 mm and inner radius of 4 mm was materialized. The tube height was chosen as 60mm (Fig. 3,4). In COMSOL's axisymmetric modelling setup, the cylinder was observed as a rectangle that was extruded 360° along the red axis r=0 (Fig 4). The base of the cylinder is given a symmetric constraint. The meshing was done for the rectangle with 218 fine rectangular mesh and 259 nodes points.

Pressure was applied inside over an area formed by a 20mm height central section of that cylinder. It resembled an area covered by an ideal pressure sensor that is applied only in that section the blue colour segment (Fig. 4). In reality, the pressure

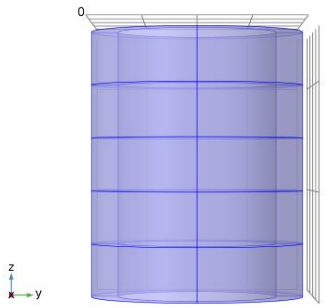

Figure 3. Cylindrical model generation from axisymmetric setup resembling length of urethra.

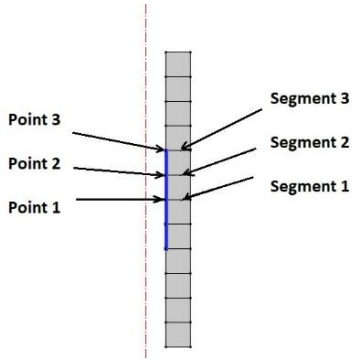

Figure 4. 'Points' and 'sections' selection on the model urethral wall. Urethra here has thickness of 5 mm and height of 60 mm. The model is axisymmetric about the red coloured axis. Pressure is applied on the inner wall, over 20 mm height highlighted in blue.

was applied on an initial area of (20*pi*4^2) mm^2. The pressure was systematically increased in steps of 1[kPa] from 0[kPa] to 120[kPa]. To describe the fibre orientation based on Gasser et al., 'curvilinear coordinates' option was used and the radial component of the fibres is set to '0'. The angles of the fibres are provided in Table 1. Curvilinear coordinates were used to describe the fibre orientation for the specified cylinder. (COMSOL, 2019).

Table 1: Gasser model parameters used

μ(kPa)	k_1 (kPa)	k_2	κ	Fibre family 1(°)	Fibre family 2(°)
5	2.5	1,5,10	0.2	40°	140°

The parameters for the simulation are given in Table 1. The same geometrical model was simulated for the same mathematical model, keeping all the parameter values same except k_2. Based on parameter variation of k_2, therefore, 3 simulation sets were created.

2.3 Circumference evaluation

'Point 1' lay on the centre of the inner wall. The other 'Points' were successively apart 5 mm from each other (Fig. 4). Inner circumference extension was plotted for the increasing pressure, for the different 'Points' on the inner part of cylinder. The outputs (curves) were compared with each other based on their slopes and values. The study was time invariant and a static evaluation was performed.

2.4 Wall Thickness evaluation

'Segment 1' lay on the central transverse section of the rectangle (Fig. 4). The other 'segments' were successively apart 5mm from each other. 'Segment 3' was the peripheral segment(boundary) of the applied load. The length of the segments was the thickness(width) of cylinder. The thickness value was evaluated through the selected pressure range for the different sections on the urethra. The outputs (curves) were compared with each other based on their slopes and values.

3. RESULTS

3.1 Circumference

The circumference at the planes(points) of the applied pressure could be seen to portray a hyperelastic response (Gasser, Ogden and Holzapfel, 2006). The circumference value at the all the measured points showed an increasing value in the entire pressure range between 0-120kPa for all the three simulations (Fig. 5-7). As seen in all the graphs, the slope of circumference change is increasing with increasing pressure, till a pressure of 10kPa. The circumferential response is stiffer post 10kPa, and all the sections provided a stronger resistance to the increasing pressure. The outermost section ('segment 3') was the portion where the circumference response looked considerably stiffer in comparison to the central and its adjacent section. Looking at the trajectory of the curve, it is possible that the circumferential stretch value for all three points within a simulation set would converge at very high input pressures.

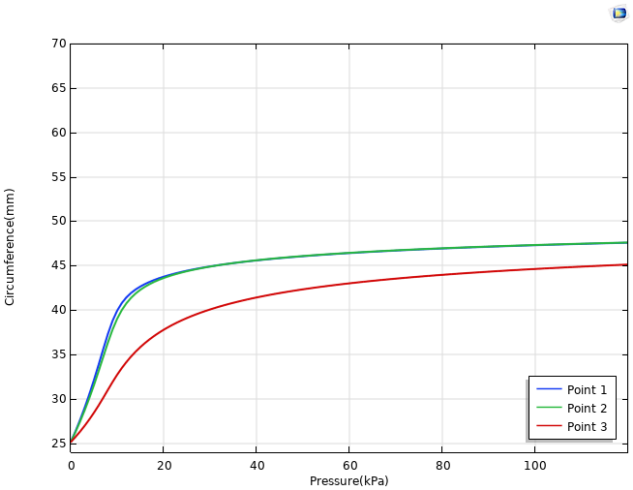

Figure 5. Pressure-circumferential values for $k_2 = 10$. The central plane (point 1) and its adjacent plane (point 2) have almost identical responses. The peripheral plane (point 3) shows a stiffer response. At 120kpa, the circumference extension measures 45mm for peripheral plane while it is 48mm for the other 2 planes.

The response circumferential stretch of points '1' and '2' within each simulation generated almost an overlapping response. Here, by simple observation, the response is slightly differentiable till pressure of 40kPa for the simulation when k_2=1 (Fig, 7). As higher values of k_2 were chosen, the pressure

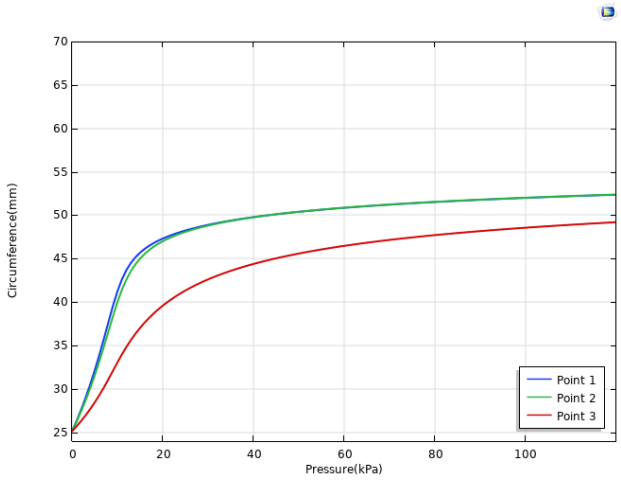

Figure 6. Pressure-circumferential values for $k_2 = 5$. The central plane (point 1) and its adjacent plane (point 2) have almost identical responses. The peripheral plane (point 3) shows a stiffer response. At 120kpa, the circumference extension measures 49mm for peripheral plane while it is 53mm for the other 2 planes.

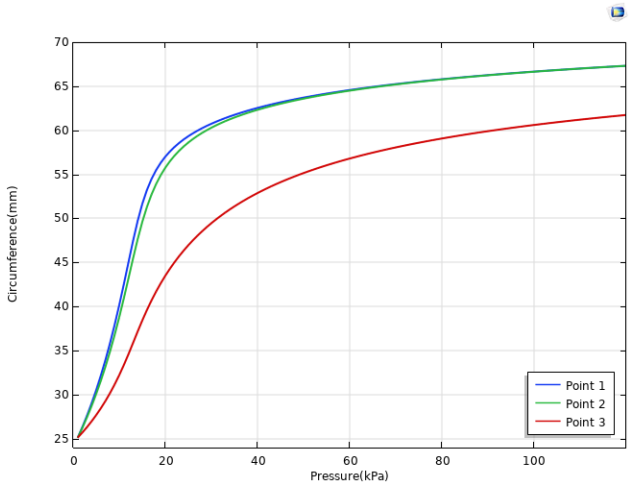

Figure 7. Pressure-circumferential values for $k_2 = 1$. The central plane (point 1) and its adjacent plane (point 2) have almost identical responses. The peripheral plane (point 3) shows a stiffer response. At 120kpa, the circumference extension measures 62mm for peripheral plane while it is 68mm for the other 2 planes.

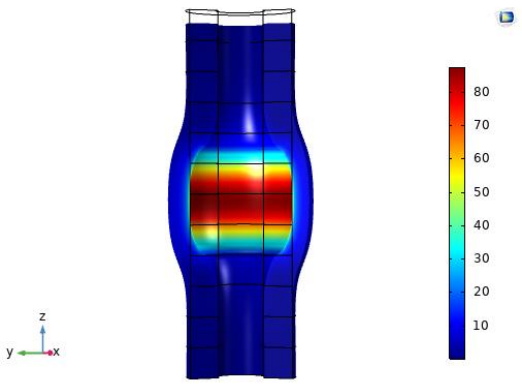

Figure 8. Deformation of cylinder for input pressure at 15 kPa and for $k_2 = 10$. Shows von-mises stresses (in kPa)

till which the response is differentiable reduced. Within any simulation, the response of 'point 3' showed a stiffer response in comparison at the other 2 points (the circumference did not extend as much as the others). Comparing the circumference value at 'point 3' in the 3 sets of simulations, it was seen that for higher values of k_2 (1, 5 and 10), the value of stretch achieved at final pressure of 120kPa reduced (62mm,49mm,45mm), respectively. As for 'points 1' and '2', a similar observation was made (68mm,53mm,48mm). The FEM tube deformation at input pressure of 15 kPa and for k_2 =10 shows von-mises stresses (Fig. 8). This example shows higher stresses in the central portion of the applied pressure.

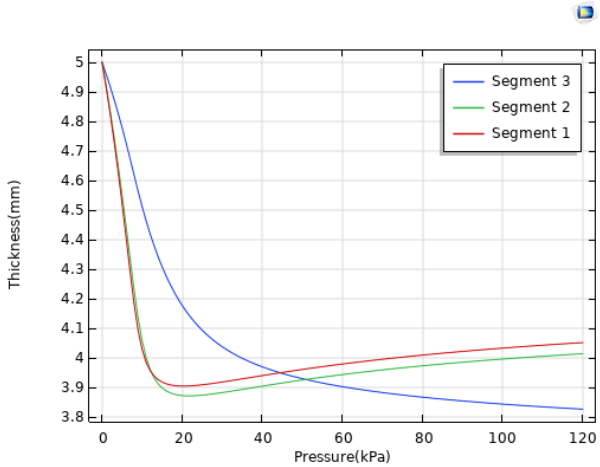

Figure 9. Thickness vs Pressure choosing k2=10. The thickness at segment 3 (peripheral plane segment) continues to reduce throughout the pressure range. The thicknesses at other 2 planes reduce faster than 'segment 3' till 15 kPa pressure, but start to slowly increase beyond that pressure.

3.2 Thickness

The original thickness(width) of each material sections were 5mm. The thickness of 'segment 3' reduced with increased application of pressure throughout the pressure range (Fig. 9). The thickness segments '1' and '2' reduced by a value of ~1.1 mm at pressure of ~20kPa (Fig. 9). From 20kPa till 120kPa, the thickness of these segments increased with a positive but decreasing slope and the increase in value was found to be ~0.1mm.

4. DISCUSSION

4.1 Circumference

All the outputs are significant, as currently, a sensor-actuator setup is being developed and identification task is being undertaken and compared and refined. Within the inflatable actuator-balloon, a thin filament like sensor in the circumferential section can provide pressure-circumference data. As such the FEM simulations show the capability to compute and display the relevant graphs for comparison later.

The model is given boundary condition that mimics the real phenomena on in-vivo inflation of the urethra when the one length of the urethra is not clamped. The FEM cylinder here is having its top surface, able to move in the z axis. When a

section of this hypothesized urethra is dilated, the circumferential changes were observed and a hyperelastic response was noted (Holzapfel, Gasser and Ogden, 2000). It is clarified here that the readings are the circumferential data obtained from point evaluation in the use of an axisymmetric model. A model clamped on both sides might give a variation in outputs.

Furthermore, from the pressure-circumference response till 10 kPa pressure (Fig. 5-7), one may observe that the plots indicate that the material becomes slightly more compliant with application of increased pressure. Beyond these pressures the tissue shows a response similar to an arterial response. This possibly could be the case with real urethral tissue, but this in-vivo data needs to be compared. The data generation was successful, but it needs to be validated and verified by real in-vivo measurements from the developed sensor-actuator outputs. It is possible to identify parameters and refine the general identification process. (Sommer and Holzapfel, 2012).

It is indicated that with higher loading pressure, the tube provided a stronger resistance to stretching and therefore circumference extended slowly (with a positive but reducing slope) (Fig. 5-7). We can observe a smoothened deformation at periphery of pressure zone (nearby 'segment 3') (Fig. 8). As we went from the central section towards the periphery, the material shows a slightly stiffer inflation characteristic. At the periphery of the input pressure region, starts the region where no pressure is applied. It is probable that the pressure from this pressured urethra zone gets transferred to the surrounding peripheral zone. The tissue has only a certain elasticity and as the pressure increases, these surrounding tissues pull the expanding tissue. However, further stress distribution discussion is not a part of this study.

As an inflatable actuator balloon is to be used to obtain the in-vivo stretching, it should be noted that the stretching in different portions of this the actuator would be different. The length of the pressured section and measurement zone would play a vital role in identification procedure. The modelling strongly suggests that an identical pressure-stretch response would not be obtained at all the sections even if the tissue properties and initial radius are identical. The geometry and the pressure region are likely the influencing factors. The amount of pre-stretch or simple force that may hold the urethra is not investigated in literature and therefore not applied here. Tissues like arteries show pre-stretches and residual stresses (Holzapfel, Gasser and Ogden, 2000). However, such studies were not available with regards to the urethra and could be part of further investigation

Considering the model parameters and its values chosen here, higher values of k_2 resulted in a stiffer material behavior. If increased to a very high value, might give pressure-circumference outputs that are not differentiable and perhaps unlike urethral tissues. Looking at the trajectory of the curves, it is possible that the final values of the circumferential extensions at all planes would converge at higher input pressures, but it needs thorough investigation. The simulated pressure limit, maybe applicable to the thin actuator but maybe not applicable directly to a real urethral tissue in-vivo owing rupturing risks (Davis *et al.*, 2018).

4.2 Thickness

As similar to the earlier section, the thickness at different planes (sections) was evaluated. Corresponding 'sections' originate from the 'points' (Fig 4). The original thickness of the material sections is 5mm (Fig. 3,4). The thickness reduces faster with increased application of pressure till 20kPa. This would likely give the indication that the material is undergoing plasticity / yielding. However, after increasing the applied pressure beyond 20kPa, it was seen that the wall thickness stopped decreasing and started increasing. The slight thickness increase till 120kPa could be attributed to the urethra tissue getting pulled into the expanding section from the surrounding areas. The thickness for the outermost section, shows gradual decrease in thickness (intensity gradually reducing) throughout the pressure range. This reinforces the hypothesis that the tissue from surrounding tissue gets pulled into the expanding zone.

This peripheral 'section 3' shows lesser expansion compared to other sections, but the thickness becomes even thinner at this area. As this region lies just on the border of the zone with applied pressure, A piercing mechanism maybe caused on this section which causes more thinning. When inserting and expanding an inflatable balloon in this regard, it needs to be understood that factors like actuator material properties and its interaction dynamics with the urethra could influence the outcomes. Inappropriate material properties of actuator or input pressures may cause excess thinning of the wall at the boundaries of urethra, thereby risking tissue damage.

5.CONCLUSION

The different values of k_2 were chosen 1,5 and 10. The purpose was to see whether a variation of this parameter generated different hyperelastic responses for the geometry chosen. It did create outputs that were dissimilar. A large dataset by varying other model parameters could be evidently obtained. The thickness at different sections as well as the stresses in the model during expansion can be successfully shown. This shows the sophisticated nature and opportunity offered by FEM simulations.

Realistic multifold geometries based on real cross section images could be created. Multiple layers and geometries based on histology can be recreated as shown initially by Holzapfel et al. A suitable mathematical model for an urethral multifold geometry is currently being investigated (Chagnon, Rebouah and Favier, 2015; Holzapfel, Gasser and Ogden, 2000).

An important identification aspect yet to be tested is 'Failure modelling'. Some studies have shown a possibility to model rupture/plasticity at high stress regions. Volokh et al. (Volokh, 2011), has implemented these simulations for consideration of arteries and used Holzapfel-Gasser-Ogden(HGO) for analytical modelling. These implementations may have not been performed on urethra considering its complex geometry and other unexplored aspects. With consideration of stricture, literature lacks biomechanical studies. Attempts are made that have incorporated these anomalies within the urethra and performed some numerical investigation (Bhave and Möller, 2021). Some studies showing urethral tissue pressure and

stretch limits were investigated and are proposed to be included as well (Davis et al., 2018).

Viscoelasticity is one of the properties of biomaterials that exhibit both viscous plus elastic characteristics when they undergo deformation. Viscoelasticity depends on the strain rate being applied on the tissue. Studies imply that the stress-strain readings taken at different times would be likely different and therefore taking the measures at inappropriate times would result in erroneous identification. A situation could arise that the biomechanical response for two biomechanically different urethra tissues would still look the same if the readings are taken at certain specific times. Incorporation of viscoelastic studies for such FEM models is not thoroughly researched and needs to be investigated further for a robust dataset (Cunnane et al., 2021; Masri et al., 2018).

ACKNOWLEDGEMENT

This research was partly supported by the German Federal Ministry of Research and Education(BMBF) under grant no. 13FH5I05IA (CoHMed/Digitalization in the OR).

AUTHOR'S STATEMENT

Authors state no conflict of interest.

REFERENCES

Bhave, A. and Möller, K. (2021) 'Urethral Stricture model to estimate overdistention of healthy tissue'. doi: 10.5281/ZENODO.4923001

Chagnon, G., Rebouah, M. and Favier, D. (2015) 'Hyperelastic Energy Densities for Soft Biological Tissues: A Review', Journal of Elasticity, 120(2), pp. 129–160. doi: 10.1007/s10659-014-9508-z

COMSOL (2019) COMSOL Multiphysics Reference Manual: https://doc.comsol.com/5.5/doc/com.comsol.help.comsol/COMSOL_ReferenceManual.pdf.

Cunnane, E.M. et al. (2021) 'Mechanical, compositional and morphological characterisation of the human male urethra for the development of a biomimetic tissue engineered urethral scaffold', Biomaterials, 269, p. 120651. doi: 10.1016/j.biomaterials.2021.120651

Davis, N.F. et al. (2018) 'Characterisation of human urethral rupture thresholds for urinary catheter inflation related injuries', Journal of the Mechanical Behavior of Biomedical Materials, 83, pp. 102–107. doi: 10.1016/j.jmbbm.2018.04.015

Dr. Ali AL-Amiri (accessed 2020) Surgery of the Penis and Urethra Chapter-.Reading.

Gasser, T.C. and Holzapfel, G.A. (2007) 'Finite Element Modeling of Balloon Angioplasty by Considering Overstretch of Remnant Non-diseased Tissues in Lesions', Computational Mechanics, 40(1), pp. 47–60. doi: 10.1007/s00466-006-0081-6

Gasser, T.C., Ogden, R.W. and Holzapfel, G.A. (2006) 'Hyperelastic modelling of arterial layers with distributed collagen fibre orientations', Journal of the Royal Society, Interface, 3(6), pp. 15–35. doi: 10.1098/rsif.2005.0073

Hampson, L.A., McAninch, J.W. and Breyer, B.N. (2014) 'Male urethral strictures and their management', Nature Reviews. Urology, 11(1), pp. 43–50. doi: 10.1038/nrurol.2013.275

Holzapfel, G.A., Gasser, T.C. and Ogden, R.W. (2000) 'A New Constitutive Framework for Arterial Wall Mechanics and a Comparative Study of Material Models', Journal of Elasticity, 61(1/3), pp. 1–48. doi: 10.1023/A:1010835316564

Masri, C. et al. (2018) 'Experimental characterization and constitutive modeling of the biomechanical behavior of male human urethral tissues validated by histological observations', Biomechanics and Modeling in Mechanobiology, 17(4), pp. 939–950. doi: 10.1007/s10237-018-1003-1

Mundy, A.R. and Andrich, D.E. (2011) 'Urethral strictures', BJU International, 107(1), pp. 6–26. doi: 10.1111/j.1464-410X.2010.09800.x

Natali, A.N. et al. (2016) 'Experimental investigation of the biomechanics of urethral tissues and structures', Experimental Physiology, 101(5), pp. 641–656. doi: 10.1113/EP085476

Sommer, G. and Holzapfel, G.A. (2012) '3D constitutive modeling of the biaxial mechanical response of intact and layer-dissected human carotid arteries', Journal of the Mechanical Behavior of Biomedical Materials, 5(1), pp. 116–128. doi: 10.1016/j.jmbbm.2011.08.013

Volokh, K.Y. (2011) 'Modeling failure of soft anisotropic materials with application to arteries', Journal of the Mechanical Behavior of Biomedical Materials, 4(8), pp. 1582–1594. doi: 10.1016/j.jmbbm.2011.01.002